Journal of Electroceramics, 13, 721–726, 2004

Gas Sensing with Perovskite-like Oxides Having ABO_3 and BO_3 Structures

V. LANTTO,[1] S. SAUKKO,[1] N.N. TOAN,[1,2] L.F. REYES,[1,3] & C.G. GRANQVIST[3]

[1]*Microelectronics and Materials Physics Laboratories, P.O. Box 4500, FIN-90014 University of Oulu, Finland*

[2]*Thin Films Physics and Technology Laboratory, Department of Microelectronic Materials, Institute of Materials Science, NCST of Vietnam, Hoang Quoc Viet Road, Gau Giay, Hanoi, Vietnam*

[3]*Department of Materials Science, The Ångström Laboratory, Uppsala University, P.O. Box 534, SE-75121 Uppsala, Sweden*

Submitted February 13, 2003; Revised March 15, 2004; Accepted March 25, 2004

Abstract. WO_3 and $LaFeO_3$ are considered as example oxides in gas sensing, respectively of perovskitelike BO_3 and ABO_3 oxide groups, the structural chemistry of which is based on corner-sharing octahedral oxygen networks where transition metal cations B occupy the octahedral cages of oxygen anioins. WO_3 is an *n*-type semiconductor and many magnetic perovskites like $LaFeO_3$ are *p*-type semiconductors. There is a great flexibility inherent in the structure of both oxide groups which gives a lot of possibilities for structure engineering of the oxides for gas-sensing applications, e.g., by a temperature treatment or by modifying with impurity atoms. We have used here a high-temperature process, advanced reactive gas deposition, to produce nanoparticle thick films of WO_3 with the metastable tetragonal crystal structure at low temperatures up to 300–400°C, and sol-gel citrate method to produce nanocrystalline $LaFeO_3$ powder as pure and modified with Sr and Mg, respectively.

Keywords: gas sensor, WO_3, $LaFeO_3$, nanocrystalline, reactive gas deposition, sol-gel

Introduction

Perovskitelike binary BO_3 and ternary ABO_3 oxides (B a transition metal) are an important group of electroceramics used for many different applications. Physical properties of interest among these oxides include *n*-type and *p*-type semiconductivity, ionic conductivity, electrochromism, colossal magnetoresistance and a multitude of dielectric, ferroelectric, piezoelectric and pyroelectric properties, which are of great importance in electronics and telecommunication. The structural chemistry of both the binary BO_3 and ternary ABO_3 oxides is based on corner-sharing octahedral oxygen networks. In the perovskite structure, the larger A cations occupy the 12-fold coordinated cuboctahedral cages of the oxygen sublattice, while the smaller B cations occupy the cages inside the oxygen octahedra. In the octahedral networks of the binary compounds, BO_3, the larger cuboctahedral cages are empty. In the metallic ReO_3, as also in the isoelectronic $NaWO_3$ bronze, the ideal cubic network structure is found at all temperatures, whereas, e.g., in WO_3 the cubic structure is newer found experimentally, but oxygen octahedra are always deformed and tilted, and the metal cation lies off-center [1]. Such distortions are a major feature of the structural chemistry of both binary and ternary compounds based on octahedral oxygen networks. Because of this great flexibility inherent in both structures, there are many different types of distortions, which can occur from the ideal cubic structure, and the physical properties of the structures depend crucially on the details of these distortions. This makes also possible to strongly modify the properties of these oxides, e.g., in the case of gas sensing, by a small amount of different additives.

We consider here gas sensing with WO_3 and $LaFeO_3$ as example oxides of BO_3 and ABO_3 oxide groups, respectively. Nanocrystalline thick films of both oxides had some gas-sensing properties which were superior to those of coarse-grained thick films [2, 3]. An advanced reactive gas deposition was used as a high-temperature route to fabricate WO_3 nanopowder [4]. High temperature during the growing process

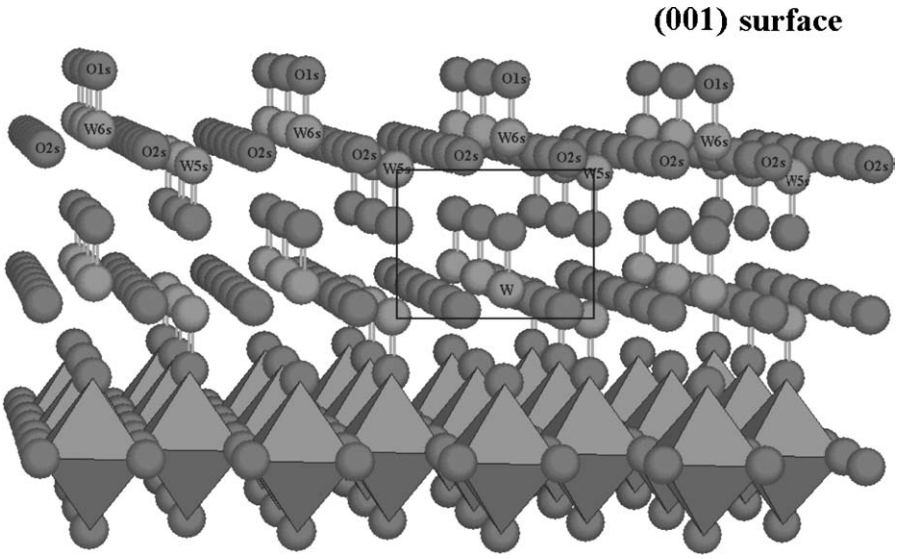

Fig. 1. Layered structure of tetragonal WO_3 with 1- and 2-fold coordinated oxygen (O1s and O2s) and 5- and 6-fold coordinated tungsten (W5s and W6s) atoms at the (001) surface. A face of the primite unit cell is also shown.

made it possible to utilize the native phase transformations of WO_3 for structure engineering of the produced nanoparticles. $LaFeO_3$ nanopowder was made by the sol-gel citrate method [3] and Sr and Mg additives were used to modify the structure and gas-sensing properties of the material.

Two Case Materials

WO_3

Our interest in the specific case of tungsten oxide was stimulated by its many applications based on its catalytic activity toward different reactions, ability to incorporate cations (secondary batteries) and form insertion compounds (the tungsten bronzes), and its electronic behaviour: it shows ferroelectric, electrochromic (smart windows), and semiconducting (semiconductor gas sensors) properties. At least, five different phases are known for WO_3. With increasing temperature, its crystal structure changes from a monoclinic low-temperature phase to a triclinic phase followed by a monoclinic room-temperature modification (8 formula units in the pseudocubic primitive cell) that is stable to about 330°C. Above that temperature, and until 740°C, the structure becomes orthorhombic, and finally, above that temperature a tetragonal phase appears up to the melting point [5]. The tetragonal phase has a layered structure perpendicular to the tetragonal *c* axis, which means a stable (001) surface structure for tetragonal crystallites, shown in Fig. 1. There are two formula units in the primitive unit cell and the structure is "antiferroelectriclike" with two opposite off-center shifts of W perpendicular to the layer in the unit cell. This layered crystal structure is very interesting from the point of view of gas sensing, since it contains terminal-like W═O bonds on both sides of each layer through the structure, in addition of surfaces, and also big 12-fold coordinated cages for ion insertion into the structure. In fact, electrochemical and optical measurements demonstrated electrochromism in the nanocrystalline tetragonal WO_3 films upon Li^+ intercalation/deintercalation [6]. In addition, an anomalous behaviour of the semiconducting gap in WO_3 was found from first-principles calculations [5]. Because of the W shifts in z-direction in the tetragonal phase, one isolated band from W5d_{xy} derived is only 0.4 eV above the top of the valence bands [5], whereas the band gap of the room-temperature monoclinic phase is about 2.5 eV.

Nanocrystalline tetragonal WO_3 films were made by reactive gas deposition using an Ultra Fine Particle equipment (ULVAC Ltd, Japan). Tungsten pellet is evaporated by induction heating at around 1150°C and oxidation in a highly laminar flow of low-pressure dry

synthetic air occurs leading to particle growth under near-equilibrium conditions with only a weak tendency towards agglomeration. The particles have a narrow size distribution [7], and it is possible to control the particle size, e.g., by the heating temperature of the tungsten pellet. WO_3 nanoparticles with the average size down to 3–4 nm were produced. The nanocrystalline WO_3 films were deposited for gas-sensing tests on alumina substrates having pre-printed gold electrodes and a Pt heating resistor printed on the reverse side.

$LaFeO_3$

Modified magnetic perovskites $LaBO_3$ with B a transition metal from Cr to Ni have been studied as a wide variety of materials for fuel cells, catalysts for automotive exhaust gas, oxidation of CO and hydrocarbons, reduction of NO_x, and for gas sensing applications [8]. Some results of nanocrystalline thick-film samples made from antiferromagnetic perovskite oxide $LaFeO_3$ (LFO) and from its two modifications $La_{0.8}Sr_{0.2}FeO_3$ (LSFO) and $LaMg_{0.1}Fe_{0.9}O_3$ (LMFO) are reported here. All these oxides had an orthorhombic crystal structure and the oxides are *p*-type semiconductors. The substitutions of Sr^{2+} for La^{3+} and Mg^{2+} for Fe^{3+} lead to changes in the values of lattice constants, oxygen content and many other properties of the base material [9, 10].

It is possible to understand some surface features of $LaFeO_3$ perovskites by considering a $(FeO_6)^{9-}$ cluster with octahedral symmetry. B-site cations exposed, e.g., to the (001) surface are missing one (or more) oxygen ligands (in fact, there are also strong distortions from the octahedral symmetry [11]). In the case of $LaFeO_3$, the cluster $(FeO_5)^{7-}$ can be used to study an approximate electronic structure at the surface where B-site cations with missing oxygen ligands provide coordinatively unsaturated d orbitals [12]. These dangling bonds produce geometrically and electronically favourable sites for chemisorption of molecules and for charge transfer between the solid and interacting molecules, which is an important factor, e.g., for C—C and C—H bond breaking in the case of catalytic reactions with hydrocarbons [13].

In the case of Sr^{2+} or Mg^{2+} ion substitution for trivalent ion sites in $LaFeO_3$, the necessary charge compensation is accomplished either by the oxidation of Fe^{3+} ions to Fe^{4+} ions or a formation of lattice oxygen vacancies. Therefore, in the modification the hole concentration increases and the conductivity of both LSFO and LMFO samples is much higher than that of the LFO sample. At the same time, sensitivity to reducing gases drastically decreases.

Nanocrystalline powders of LFO, LSFO and LMFO were synthesized by the sol-gel citrate method and the nanocrystalline oxides were obtained after calcining the powders for 2 h at 500–700°C. The average crystallite sizes, calculated from the line widths of the (110) reflection peaks of the X-ray diffraction patterns, were 27, 16 and 14 nm, respectively, for LFO, LSFO and LMFO powders. The thick-film samples were screen printed from the powders on similar alumina substrates as in the case of WO_3 samples.

Gas Sensing Results

WO_3 Samples

Some results are given here for a tetragonal nanoparticle WO_3-film sample sintered at 300°C after deposition. The average particle size of the film was ~10 nm. The conductance of the sample as a function of inverse tempareture in dry synthetic air is shown in the insert of Fig. 2. During heating, the conductance starts to increase from the room-temperature value of about 5 nS and above about 400 K the increase is exponential with an activation energy of about 0.4 eV which is the value of the band gap calculated for tetragonal WO_3 in Ref. 5. After mixing of 5 and 10 ppm of H_2S with the dry synthetic air, the conductance increases at room temperature by factors of about 250 and 2000, respectively, as shown in the insert in Fig. 2. The maximum sensitivity of the sample to both 5 and 10 ppm of H_2S in dry air is at about 400 K where the conductance curves in Fig. 2 have sharp maximums. In addition, shoulders are shown in both conductance curves around about 470 K and also in the Arrhenius plots (a small shoulder also in the plot for dry air) in the insert in Fig. 2. It is also seen that the H_2S sensitivity of the sample is small above about 600 K where the conductance values again start to increase with increasing temperature.

LFO, LSFO and LMFO Samples

The temperature dependence of conductance of LFO and LSFO samples in dry synthetic air and also in gas

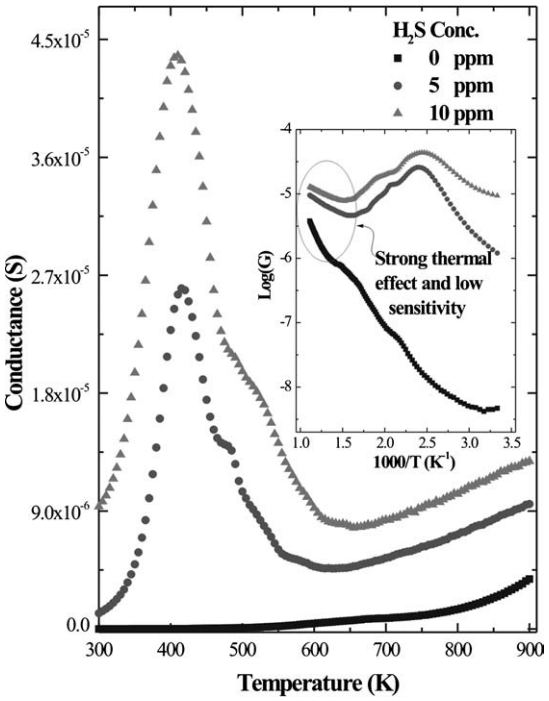

Fig. 2. Conductance of a tetragonal WO_3-film sample sintered at 300°C as a function of temperature in dry synthetic air mixed with 0, 5 and 10 ppm of H_2S, respectively. The Arrhenius plots of the three conductance curves are shown in the insert.

mixtures containing 200 ppm of CO, CH_4 and C_2H_4, respectively, in dry air are shown in Fig. 3. The conductance behaviour in these Arrhenius plots is interesting, especially, in the case of the LFO sample. At low temperatures, all three reducing gases increase the conductance of the samples having *p*-type semiconducting films, whereas at higher temperatures the situation is reversed and the highest conductance values are in dry air. Usually, a reducing gas like CO decreases the conductance of a *p*-type semiconductor. In the case of the LFO sample in Fig. 3(a), the border temperatures T* for these dual conductance responses [14] are at about 180°C for CH_4, 200°C for C_2H_4 and 240°C for CO. The average activation energies of conductances in the case of the LSFO sample in Fig. 3(b) are smaller as compared with those of the LFO sample in Fig. 3(a). In addition, the conductance values are much larger and, respectively, the relative conductance responses to all three reducing gases much smaller for the LSFO sample in Fig. 3(b). The conductance of the LMFO sample was two orders of magnitude smaller than that of the LSFO sample at room temperature, and the average activation energies and relative conductance responses of the LMFO sample were between those obtained for LFO and LSFO samples in Figs. 3(a) and (b), respectively.

A survey of the gas response behaviour of a relatively large group of semiconducting oxides was given by Moseley et al. [15], however, not including $LaFeO_3$. In their survey and classification of gas responses they also describe [15, 16] the unusual dual conductance behaviour for some semiconducting oxides (they call it 'transition between *n*-type and *p*-type behaviour'). The dual conductance response at exposure to CO was found also in the case of *n*-type CdS and α-$SnWO_4$ thin films by Solis et al. [14, 17]. The α-$SnWO_4$ thin films were grown by means of reactive co-sputtering from tin and tungsten targets. However, α-$SnWO_4$ thick films made by screen printing from powders did not show the dual conductance response at exposure to CO and other reducing gases [18, 19].

It was argued in Ref. 14 that the origin for the dual conductance response is at the film surfaces. E.g., in the case of CO, a possibility is that CO behaves as a surface acceptor trapping electrons to its antibonding $2\pi^*$ orbital. Then, it behaves as an oxidizing gas decreasing the conductance of an *n*-type semiconductor like α-$SnWO_4$ and increasing the conductance of a *p*-type semiconductor like $LaFeO_3$. The results obtained by structural characterization of α-$SnWO_4$ thin and thick films using x-ray diffraction, Mössbauer spectroscopy, Raman spectroscopy, infrared spectroscopy, optical spectroscopy, Rurherford backscattering spectroscopy, scanning electron microscopy and atomic force microscopy [14, 17–21] support to the reasoning that sensing film surfaces have an important role for the dual conductance response. Changes in polar surface layers of ionic semiconductors and corresponding changes in the electron affinity of the semiconductor may also relate to the dual conductance behaviour [22]. In addition, interfacial oxide layers at the electrode-oxide phase boundary [23] may play a role in the dual conductance behaviour.

Especially, the oxidizing behaviour of CO gives a strong conductance increase of the $LaFeO_3$ sample at low temperatures in Fig. 3(a). At exposure to 200 ppm of CO at 100°C, the conductance increases by a factor of ∼300, and already at room temperature there is a notable increase of conductance in Fig. 3(a). This can be compared to the CO response of SnO_2

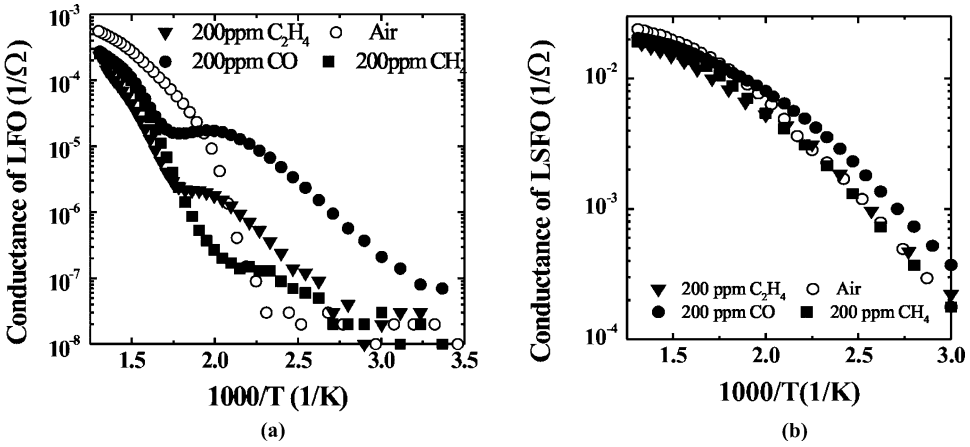

Fig. 3. Temperature dependence of conductance of (a) LFO and (b) LSFO samples in dry synthetic air and at exposure to 200 ppm of CO, CH_4 and C_2H_4 in synthetic air, respectively.

thick films in synthetic air where conductance increase starts to appear not until above ∼280°C. In the case of CH_4 exposure, still higher temperatures are needed with SnO_2 samples. An easy electron transfer from the dangling bonds of Fe cations with missing oxygen ligands at $LaFeO_3$ surfaces to CO is an explanation for CO chemisorption and high conductance increase of *p*-type $LaFeO_3$ samples at exposure to CO at low temperatures.

Conclusions

Nanoparticle thick films of WO_3 with the metastable tetragonal (layered) crystal structure were found to be very sensitive to H_2S already at room temperature without any heating. Terminal double-bonded oxygen on the layered surfaces of tetragonal WO_3 together with an exceptionally small band gap of tetragonal WO_3 [5] may have something to do with the specific sensing properties of the tetragonal WO_3 films. The modification of $LaFeO_3$ by Sr and Mg had an effect to strongly increase the conductance of the nanocrystalline thick-film samples. At low operation temperatures of the samples, an exceptional dual conductance response was found at exposure to the tested reducing gases CO, C_2H_4 and CH_4. In the case of CO exporure, a high conductance increase of the $LaFeO_3$ sample was found at low operation temperatures, e.g., by a factor of ∼ 300 at exposure to 200 ppm of CO in synthetic air at 100°C. The sensitivity of the LMFO and LSFO samples was much lower than that of the LFO sample at exposure to CO, C_2H_4 and CH_4.

References

1. F. Cora, A. Patel, N.H. Harrison, R. Dovesi, and C.R.A. Catlow, *J. Am. Chem. Soc*., **118**, 12174 (1996).
2. J.L. Solis, S. Saukko, L. Kish, C.G. Granqvist, and V. Lantto, *Thin Solid Films*, **391**, 255 (2001).
3. N.N. Toan, S. Saukko, and V. Lantto, *Physica B*, **327**, 279 (2003).
4. J.L. Solis, A. Hoel, L.B. Kish, C.G. Granqvist, S. Saukko, and V. Lantto, *J. Am. Ceram. Soc*., **84**(7), 1501 (2001).
5. G.A. de Wijs, P.K. de Boer, and R.A. de Groot, *Phys. Rev. B*, **59**(4), 2684 (1999).
6. J.L. Solis, A. Hoel, V. Lantto, and C.G. Granqvist, *J. Appl. Phys*., **89**, 2727 (2001).
7. J. Söderlund, L.B. Kiss, G.A. Niklasson, and C.G. Cranqvist, *Phys. Rev. Lett*., **80**(11), 2386 (1998).
8. G. Martinelli, M.C. Carotta, M. Ferroni, Y.Sadaoka, and E. Traversa, *Sens. Actuators B*, **55**, 99 (1999).
9. P. Porta, S. Cimino, S. de Rossi, M. Faticanti, G. Minelli, and I. Pettiti, *Mater. Chem. Phys.*, **71**, 165 (2001).
10. P. Ciambelli, S. Cimino, S. de Rossi, L. Lisi, G. Minelli, P. Porta, and G. Russo, *Appl. Catal. B: Environmental,* **29**, 239 (2001).
11. N. Erdman, K.R. Poeppelmeler, M. Asta, O. Warschkow, D.E. Ellis, and L.D. Marks, *Nature*, **419**, 55 (2002).
12. I. Kojima, H. Adachi, and I. Yasumori, *Surface Science*, **130**, 50 (1983).
13. T. Arakawa, H. Kurachi, and J. Shiokawa, *J. Materials Science*, **20**, 1207 (1985).
14. J. L. Solis, V. Golovanov, V. Lantto, and S. Leppävuori, *Physica Scripta*, **T54**, 248 (1994).
15. P.T. Moseley, A.M. Stoneham, and D.E. Williams, in*Techniques and Mechanisms in Gas Sensing*, edited by P.T. Moseley, J.O.W.

Norris, and D.E. Williams (Adam Hilger, Bristol, New York, 1991), pp. 108–138.
16. P.T. Moseley, *Sens. Actuators B*, **3**, 167 (1991).
17. J.L. Solis and V. Lantto, *Sens. Actuators B,* **24**/**25**, 591 (1995).
18. J.L. Solis and V. Lantto, *Physica Scripta*, **T69**, 281 (1997).
19. J.L. Solis, V. Lantto, L.Häggström, and M. Wikner, *Hyperfine Interactions C,* **2**, 256 (1997).
20. J.L. Solis, J. Frantti, V. Lantto, L.Häggström, and M. Wikner, *Phys. Rev. B,* **57**, 13491 (1998).
21. J.L. Solis, J. Frantti, V. Lantto, L.Häggström, and M. Wikner, *Physica Scripta*, **T79**, 216 (1999).
22. V. Lantto, T.S. Rantala, and T.T. Rantala, *Electron Technology*, **33**, 22 (2000).
23. F.P. Netzer, *Surface Review and Letters*, **9**, 1553 (2002).